LBL-19098 c.2

LBL-19098

Presented at the Polymer Processing Society Conference, Akron, OH, March 28, 1985

PROFILE DEVELOPMENT IN DRAWN HOLLOW TUBES

B.D. Freeman, M.M. Denn, R. Keunings, G.E. Molau, and J. Ramos

February 1985

RECEIVED
LAWRENCE
BERKELEY LABORATORY

APR 17 1985

LIBRARY AND
DOCUMENTS SECTION

TWO-WEEK LOAN COPY

This is a Library Circulating Copy
which may be borrowed for two weeks.

Lawrence Berkeley Laboratory
University of California
Berkeley, California 94720

Prepared for the U.S. Department of Energy
under Contract DE-AC03-76SF00098

Center for Advanced Materials

LBL-19098 c.2

DISCLAIMER

This document was prepared as an account of work sponsored by the United States Government. While this document is believed to contain correct information, neither the United States Government nor any agency thereof, nor the Regents of the University of California, nor any of their employees, makes any warranty, express or implied, or assumes any legal responsibility for the accuracy, completeness, or usefulness of any information, apparatus, product, or process disclosed, or represents that its use would not infringe privately owned rights. Reference herein to any specific commercial product, process, or service by its trade name, trademark, manufacturer, or otherwise, does not necessarily constitute or imply its endorsement, recommendation, or favoring by the United States Government or any agency thereof, or the Regents of the University of California. The views and opinions of authors expressed herein do not necessarily state or reflect those of the United States Government or any agency thereof or the Regents of the University of California.

PROFILE DEVELOPMENT IN DRAWN HOLLOW TUBES

B.D. Freeman, M.M. Denn, and R. Keunings

Center for Advanced Materials
Lawrence Berkeley Laboratory
and
Department of Chemical Engineering
University of California
Berkeley, California 94720

and

G.E. Molau and J. Ramos

Dow Chemical U.S.A.
Walnut Creek, California 94598

ABSTRACT

Profile development in isothermal drawing of hollow tubes is studied using finite-element and asymptotic analyses. The transition from die flow to extensional flow of an annulus occurs over a distance comparable to the annular thickness. Considerable extrudate swell can occur with the flow rearrangement, and the final ratio of inner to outer radius can fall below that at the die despite an increase in this ratio over the entire draw zone. Asymptotic "thin-filament" equations describe the flow beyond the region of flow rearrangement.

INTRODUCTION

The extrusion and drawing of hollow tubes from molten polymers is similar to the process of extrusion and drawing of textile fibers, in that there are three distinct regions that must be analyzed: the region of shear flow and profile rearrangement in and near the die or spinneret, the melt drawing region, and the region near the point of solidification. The major difference between the two processes is the additional degree of freedom afforded by the ability to impose an internal pressure in the hollow tube. This additional degree of freedom makes it possible in principle to control both the outer and inner radii of the drawn hollow tube.

The melt drawing region for textile fibers has been analyzed using an asymptotic analysis known as the thin filament equations. These equations are not valid in the region of flow rearrangement and extrudate swell near the spinneret, and finite-element methods have been used to study the flow in that region. The general conclusion is that the two methods give comparable results in the region of overlap, thus validating the use of the asymptotic analysis and establishing the appropriate initial state for the thin filament equations. These approaches to the simulation of fiber spinning are discussed in a recent chapter on computational methods (Denn, 1984), where complete references may be found. Little has been done regarding the solidification region, and most simulations take solidification to occur instantaneously, without any enthalpy change, at a specified temperature.

We describe here analyses of the rearrangement and melt drawing regions of hollow tubes. The approach is similar to that used for textile fibers, except that the asymptotic analysis is modified by the presence of the internal pressure and the finite element treatment must deal with two free

surfaces. One important conclusion with regard to processing is that the annular extrudate swell makes the rearrangement region more important in this process than in textile fiber spinning.

FORMULATION

The hollow tube is shown schematically in Fig. 1. For axi-symmetric steady flow the equations for conservation of mass and momentum are as follows:

$$\frac{1}{r}\frac{\partial}{\partial r}(\rho r v_r) + \frac{\partial}{\partial z}(\rho v_z) = 0 \tag{1}$$

$$\rho\left(v_r \frac{\partial v_r}{\partial r} + v_z \frac{\partial v_r}{\partial z}\right) = -\frac{\partial p}{\partial r} + \frac{1}{r}(r\tau_{rr}) - \frac{\tau_{\theta\theta}}{r} + \frac{\partial \tau_{rz}}{\partial z} \tag{2a}$$

$$\rho\left(v_r \frac{\partial v_z}{\partial r} + v_z \frac{\partial v_z}{\partial z}\right) = -\frac{\partial p}{\partial z} + \frac{1}{r}\frac{\partial}{\partial r}(r\tau_{rz}) + \frac{\partial \tau_{zz}}{\partial z} + \rho g \tag{2b}$$

v_r and v_z are the r-and z- components, respectively, of the velocity vector $\underset{\sim}{v}$. g is the gravitational acceleration; the drawing direction is assumed to be vertical. τ_{ij} is the extra-stress, and p is the isotropic pressure; the total stress σ_{ij} is

$$\sigma_{ij} = -p\delta_{ij} + \tau_{ij} \tag{3}$$

where δ_{ij} equals unity when i and j are the same, and zero otherwise.

There are free-surface boundary conditions on both the velocity and the stress. The velocity condition is that there be no flow through the surface, or $\underset{\sim}{n}\cdot\underset{\sim}{v} = 0$ at $r = R_o$ and R_i; this is equivalent to

$$v_r = R_o' v_z \text{ at } r = R_o \tag{4a}$$

$$v_r = R_i' v_z \text{ at } r = R_i \tag{4b}$$

where R' denotes $\frac{dR}{dz}$. The stress conditions are most easily expressed in terms of the tangential and normal tractions, $\underset{\sim}{\sigma}_n$ and $\underset{\sim}{\sigma}_t$, respectively:

$$\underset{\sim}{\sigma}_n = \underset{\sim}{0} \ , \ \underset{\sim}{\sigma}_t = -\rho_a |\underset{\sim}{v} - \underset{\sim}{v}_a| C_D^2 \text{ at } r=R_o \tag{5a}$$

$$\underset{\sim}{\sigma}_n = -p_i \ , \ \underset{\sim}{\sigma}_t = \underset{\sim}{0} \text{ at } r=R_i \tag{5b}$$

$\underset{\sim}{v}_a$ and ρ_a are the velocity and density of the ambient air, and C_D is an air-drag coefficient. p_i is the internal pressure.

The temperature field is assumed to be axi-symmetric, axial conduction is neglected relative to convection, radial convection is neglected relative to conduction, and dissipation is assumed to be negligible. The energy equation is then

$$\rho v_z c_p \frac{\partial T}{\partial z} = k \frac{1}{r} \frac{\partial}{\partial r} \left(r \frac{\partial T}{\partial r} \right) \tag{6}$$

There is no heat transfer to the inner core, while heat transfer to ambient air at temperature T_a is described by a heat transfer coefficient, h. The boundary conditions are therefore

$$\frac{\partial T}{\partial r} = 0 \text{ at } r=R_i \tag{7a}$$

$$-k \frac{\partial T}{\partial r} = h(T-T_a) \text{ at } r=R_o \tag{7b}$$

THIN FILAMENT EQUATIONS

The thin filament equations are obtained by averaging Eqs. (1) and (2) over the cross-section at each value of z. The average $\bar{\psi}(z)$ of a variable $\psi(r,z)$ is defined as

$$\bar{\psi}(z) = \frac{1}{\pi(R_o^2 - R_i^2)} \int_{R_i}^{R_o} 2\pi r \psi(rz) dr \tag{8}$$

In computing derivatives with respect to z of averaged quantities, it is important to recall that both limits of integration are functions of the independent variable.

In averaging Eqs. (1) and (2) the following approximations are required, where $\bar{v}$ denotes $\overline{v_z}$:

(i) $\frac{dR_o}{dz}, \frac{dR_i}{dz} << 1$

(ii) $\overline{v_z^2} \approx \bar{v}^2$

(iii) $\frac{d}{dz} \int_{R_i}^{R_o} 2\pi r^2 \tau_{rz} dr \approx 0$

(iv) inertial term can be neglected in the r-component of the averaged momentum equation.

Averaging of the continuity and z-momentum equations is straightforward. The r-component of momentum is averaged by multiplying each term by $2\pi r^2$ and integrating $^-$ rather than by $2\pi r^-$, because of the r^{-1} that appears in most terms. Averaging of the convection term in Eq. (6) requires the assumption that v_z and the physical properties are independent of r. The resulting thin filament equations are then as follows:

$$w = \pi(R_o^2 - R_i^2)\rho\bar{v} = \text{constant} \tag{9}$$

$$w\frac{d\bar{v}}{dz} = \frac{d}{dz}\left\{\pi(R_o^2 - R_i^2)\left[\bar{\tau}_{zz} - \frac{1}{2}(\bar{\tau}_{rr} + \bar{\tau}_{\theta\theta})\right]\right\} - \pi R_o \rho_a \bar{v}^2 C_D + \pi(R_o^2 - R_i^2)\rho g \tag{10}$$

$$\frac{R_o R_i}{R_o^2 - R_i^2} p_i = \frac{1}{2} (\bar{\tau}_{\theta\theta} - \bar{\tau}_{rr}) \tag{11}$$

$$w\, c_p \frac{d\bar{T}}{dz} = -\, 2\pi h R_o (T - T_a) \tag{12}$$

$$\bar{\sigma}_{zz} = \frac{R_i^2}{R_o^2 - R_i^2} p_i + \bar{\tau}_{zz} - \frac{1}{2} (\bar{\tau}_{rr} + \bar{\tau}_{\theta\theta}) \tag{13}$$

Equations (9), (10), and (12) are identical to the thin filament equations for textile fibers, except for the replacement of R^2 by $R_o^2 - R_i^2$ to account for the hollow center. Equation (11) accounts for the hoop stress resulting from the internal pressure, and is required in order to provide an independent equation for the additional variable in the hollow tube process. It is to be noted that in general $\bar{\tau}_{\theta\theta} \neq \bar{\tau}_{rr}$.

INELASTIC LIQUIDS

A constitutive equation for the extra-stress is required in order to complete the description. Here the kinematical assumption $v_z = \bar{v}(z)$ must be made explicitly. The average stresses are then computed as follows for an inelastic liquid in which the only rheological parameter is a single non-Newtonian viscosity:

$$\bar{\tau}_{zz} - \frac{1}{2} \left(\bar{\tau}_{rr} + \bar{\tau}_{\theta\theta}\right) = 3\eta \frac{d\bar{v}}{dz} \tag{14}$$

$$\bar{\tau}_{\theta\theta} - \bar{\tau}_{rr} = -\, \frac{4\eta\, \ln (R_i/R_o)}{R_o^2 - R_i^2} \frac{d}{dz} (R_i^2 \bar{v}) \tag{15}$$

ANALYTICAL RESULTS

Many of the analytical solutions to the thin filament equations for textile fiber spinning apply without change to the equations for drawn hollow tubes. For isothermal, low speed (no inertia or air drag) drawing of a Newtonian hollow tube without significant gravitational force the velocity varies exponentially with distance,

$$\bar{v} = v_o \exp\left(\frac{Bz}{r_o - r_i}\right) \tag{16}$$

$$B = \frac{F - \pi r_i^2 P_i}{3\pi\eta V_o (r_o + r_i)} \tag{17}$$

Here r_o and r_i are the values of the inner and outer radius, respectively, at $z=0$, and v_o is the average velocity at $z=0$. F is the tensile force applied to draw the hollow tube. Clearly the relative importance of the internal pressure is governed by the dimensionless ratio $\pi r_i^2 p_i/F$; drawdown will be very slow as this group becomes of order unity, and the tube wall will thicken for values greater than unity. The asymptotic solutions for low speed, isothermal spinning of a Maxwell fluid (Den et al., 1976) similarly apply, with a linear velocity profile and a maximum drawdown in the limit of large applied force.

One of the immediate consequences of Eqs. (9), (11), and (15) for $p_i > 0$ is

$$\frac{d}{dz}\left(\frac{R_i}{R_o}\right) > 0 \tag{18}$$

This is of particular processing significance, since control of R_o and R_i individually is important. It is found experimentally, in fact, that R_i/R_o in a drawn thin hollow filament is about twenty percent <u>less</u> than the value at

the die. We shall return to this point in the discussion of profile rearrangement near the die.

A further consequence of these equations is that, when $p_i = 0$, both $R_i^2 \bar{v}$ and $R_o^2 \bar{v}$ must remain constant. This result is useful as a check on the internal consistency of computational algorithms.

Finally, with standard correlations for the heat transfer coefficient Eq. (12) for the temperature is insensitive to the kinematics, and the approximate solution given by Fisher and Denn (Denn, 1984) for the temperature profile and the point of solidification will apply directly for moderate drawdowns.

HOLLOW FIBER SPINNING

A typical simulation using the thin filament equations is illustrated in Figs. 2 and 3. The polymer properties were taken to be those of 0.67I.V. poly(ethylene terephthelate), with the temperature-equivalent Newtonian viscosity given by Gregory. Kase and Matsuo's heat transfer coefficient was used, and Matsuo's correlation for air drag were used (Denn, 1984). The relevant operating parameters are given in Table 1. The general shapes of the velocity and temperature profiles are typical of those computed for the spinning of PET fibers. The very large area reduction ratios and relatively slow spinning speeds are typical of hollow fiber processing. The takeup speed is in the range where inertial and air drag effects are first expected to influence the profile development, and the force in fact varies by only about 10 percent over the length of the draw zone. The factor $\pi r_i^2 p_i/F$ (using the value of F at z=0) is only equal to 0.018, so the internal pressure has little effect on the profile development and R_i/R_o increases only slightly over the length of the draw zone.

Input Variables	
Extrusion temperature	295°C
Solidification temperature	70°C
Ambient air temperature	30°C
Quench air velocity	0.2 m/s
Throughput	6.8 mm^3/s
Spinneret dimensions, r_o	1.0 mm
r_i	0.6 mm
Internal pressure, p_i	27 Pa
Takeup speed	14 m/s
Area reduction ratio	4140

Computed Variables	
Spinneret stress	0.845 kPa
Takeup stress	3825 kPa
B	0.17
$\pi r_i^2 p_i/F$	0.018

Table 1
Variables for simulation of melt spinning of a poly(ethylene terephthalate) hollow fiber

FINITE ELEMENT CALCULATIONS

Behavior in the region near the spinneret was analyzed by obtaining numerical solutions to Eqs. (1) and (2) using POLYFLOW(R), a finite element code developed at the Université Catholique de Louvain for the numerical simulation of viscoelastic flows (Crochet, 1982). The code is based on algorithms proposed in Crochet and Keunings (1980, 1982) and Keunings and Crochet (1984) and described in detail by Crochet et al. (1984). Although POLYFLOW(R) has nonisothermal capabilities, the solution was carried out only for isothermal flow and is therefore restricted to the region very close to the die where significant heat transfer will not yet have taken place. Because of the slow speeds in this region there is no need to include inertia or the air drag boundary condition.

Some typical calculations for a Newtonian fluid are shown in Figs. 4 through 6 for $r_i/r_o = 0.6$. The exponential velocity profile is achieved within one unit of distance, measured in units of the annular die thickness r_o-r_i, and the slope of the plot of $\ln \bar{v}$ versus $z/(r_o-r_i)$ is equal to B as defined in Eq. (16); thus, the validity of the thin filament equations for the draw zone is established. As in the case of textile fiber spinning (Keunings et al., 1983), the asymptotic solutions extrapolate approximately to the velocity corresponding to free extrudate swell (no imposed force), so this velocity could be used as the initial condition for the thin filament equations.

The several effects governing the rearrangement region for the hollow fiber are illustrated in Fig. 5 with reference to the inner radius. R_i initially decreases because of extrudate swell. (Since R_o increases because of extrudate swell at the same time, $d(r_i/r_o)/dz$ must be negative in this

region.) The positive internal pressure then causes R_i to increase. Finally, as the drawdown takes effect, R_i begins to decrease monotonically down the spinline. (It should be noted that the thin filament equations admit an initially increasing R_i, followed by a maximum, for a sufficiently large internal pressure.) The effect of internal pressure on the ratio r_i/r_o, as shown in Fig. 6, is substantially greater than the effect on the velocity and stress profiles.

The conditions in Table 1 were simulated using POLYFLOW(R), taking the poly(ethylene terephthalate) to be Newtonian with all physical properties at the spinneret temperature. The results are shown in Figs. 7 and 8, together with the solution of the non-isothermal thin filament equations. The initial conditions for the for the thin filament equations were taken from the finite element solution at 0.3 mm, or 0.75 (r_o-r_i), from the die. The curves should deviate because the asymptotic analysis accounts for the changing physical properties with temperature. As would be expected, the initial slopes of the velocity profiles are the same, and the profiles are in close agreement over about 3 mm, or 7.5 (r_o-r_i). The radius ratios deviate much more rapidly, though the qualitative behavior is the same.

Figure 8 illustrates what is perhaps the most important processing result from this study. The initial extrudate swell is the most important factor in determining the ultimate ratio R_i/R_o on a drawn hollow fiber. For the parameters used here this ratio is computed to be at or below the die ratio r_i/r_o, despite the fact that $d(R_i/R_o)/dz$ is positive over most of the length of the hollow fiber spinline. The stresses, however, and hence the structure, are developed in the draw zone.

The recoverable shear in the die for the conditions in Table 1 is 0.13, based on Gregory's relaxation time estimates for poly(ethylene terephthalate).

This is a low level of viscoelasticity, and Keunings et al. (1983) saw only small effects at this level near the spinneret in textile fiber spinning; Gagon and Denn (1981) found that there were spinning conditions where the thin filament equations did show markedly different behavior between Newtonian and viscoelastic descriptions of poly(ethylene terephthalate) rheology. The conditions in Table 1 were simulated with POLYFLOW(R) using an Oldroyd B fluid model (Crochet and Keunings, 1982), with a viscosity ratio of 1/9 and a recoverable shear of 0.13. The computed velocity profiles for the Newtonian and Oldroyd B fluids were essentially the same. The difference was more apparent in the ratio r_i/r_o, however, as shown in Fig. 9, since this ratio is sensitive to small differences in extrudate swell.

CONCLUSION

A complete analysis of the drawing of hollow tubes requires detailed consideration of the region of flow rearrangement near the die, as well as stress and area development in the draw region. The asymptotic thin filament equations for the latter predict average velocity and temperature profiles similar to those found previously for textile fibers. The evolution of the ratio of inner to outer radius in the draw region is governed by the extrudate swell, which will be sensitive to fluid rheology.

ACKNOWLEDGMENTS

This work was supported by the Director, Office of Energy Research, Office of Basic Energy Sciences, Materials Sciences Division of the U.S. Department of Energy under Contract No. DE-AC03-76SF00098. B.D. Freeman was a Berkeley Fellow and a National Science Foundation Fellow during the period of this work. M.M. Denn was a Visiting Professor at the University of Melbourne Chemical Engineering Department during the period of manuscript preparation. We are grateful to Prof. Marcel Crochet for making POLYFLOW(R) available at the University of California, Berkeley, and to Dow Chemical U.S.A. for permission to include the work done at Dow.

REFERENCES

M.J. Crochet, "POLYFLOW, a Finite Element Program for the Simulation of Viscoelastic Flow: Theoretical Background" (1982) Unité de Mechanique Appliquée, Université Catholique de Louvain.

M.J. Crochet and R. Keunings, J. Non-Newtonian Fluid Mech. 7 (1980) 198.

M.J. Crochet and R. Keunings, J. Non-Newtonian Fluid Mech. 10 (1982) 339.

M.J. Crochet, A.R. Davies, and K. Walters, "Numerical Simulation of Non-Newtonian Flow," (1984), Elsevier, Amsterdam.

M.M. Denn, "Fiber Spinning," in J.R.A. Pearson and S. Richardson, eds., "Computational Analysis of Polymer Processing," (1983), Applied Sci. p.51, London.

M.M. Denn, C.J.S. Petrie, and P. Avenas, AIChE J. 21 (1975) 795.

D.K. Gagon and M.M. Denn, Polymer Eng. & Sci. 21 (1981) 844.

D.R. Gregory, Trans. Soc. Rheology 17 (1973) 191.

R. Keunings and M.J. Crochet, J. Non-Newtonian Fluid Mech. 14 (1984) 279.

R. Keunings, M.J. Crochet, and M.M. Denn, Ind. Eng. Chem. Fundamentals 22 (1983) 347.

CAPTIONS FOR FIGURES

Fig. 1 Schematic of a drawn hollow tube.

Fig. 2 Velocity profile from thin filament equations for conditions in Table 1.

Fig. 3 Temperature profile from thin filament equations for conditions in Table 1.

Fig. 4 Effect of internal pressure on velocity profile, finite element computation. $r_o = 1.0$, $r_i = 0.6$, $F = 2.0$, $v_o = 1.6$, $\eta = 1.0$.

Fig. 5 Effect of internal pressure on development of R_i for conditions in Fig. 4.

Fig. 6 Effect of internal pressure on the ratio R_i/R_o for conditions in Fig. 4.

Fig. 7 Velocity profile development for conditions in Table 1.

Fig. 8 Ratio R_i/R_o for conditions in Table 1.

Fig. 9 Effect of viscoelasticity in ratio R_i/R_o for conditions in Table 1.

FIGURE 1.

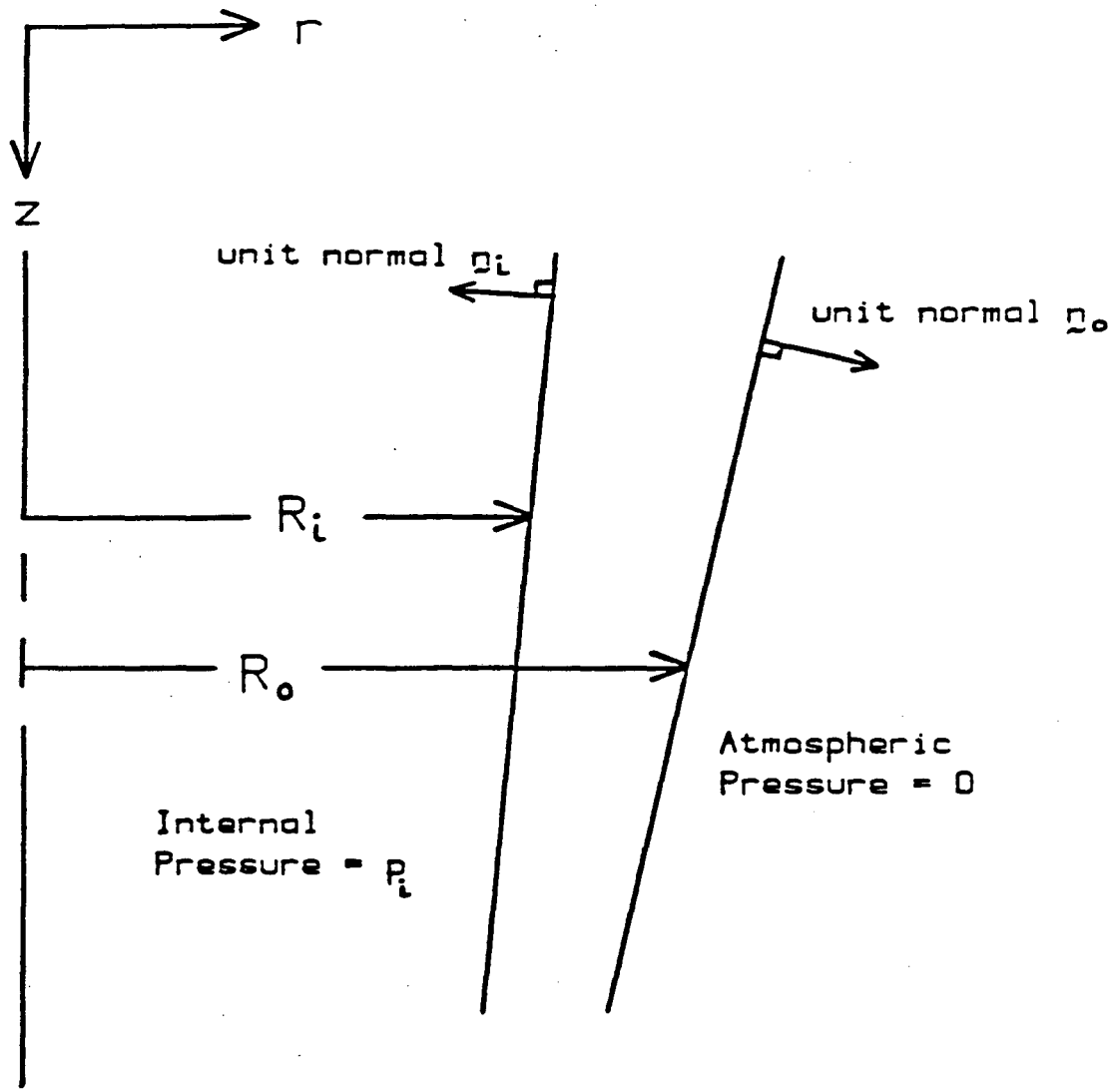
r
z
unit normal $\underset{\sim}{n}_i$
unit normal $\underset{\sim}{n}_o$
R_i
R_o
Atmospheric
Pressure = 0
Internal
Pressure = p_i

FIGURE 2.

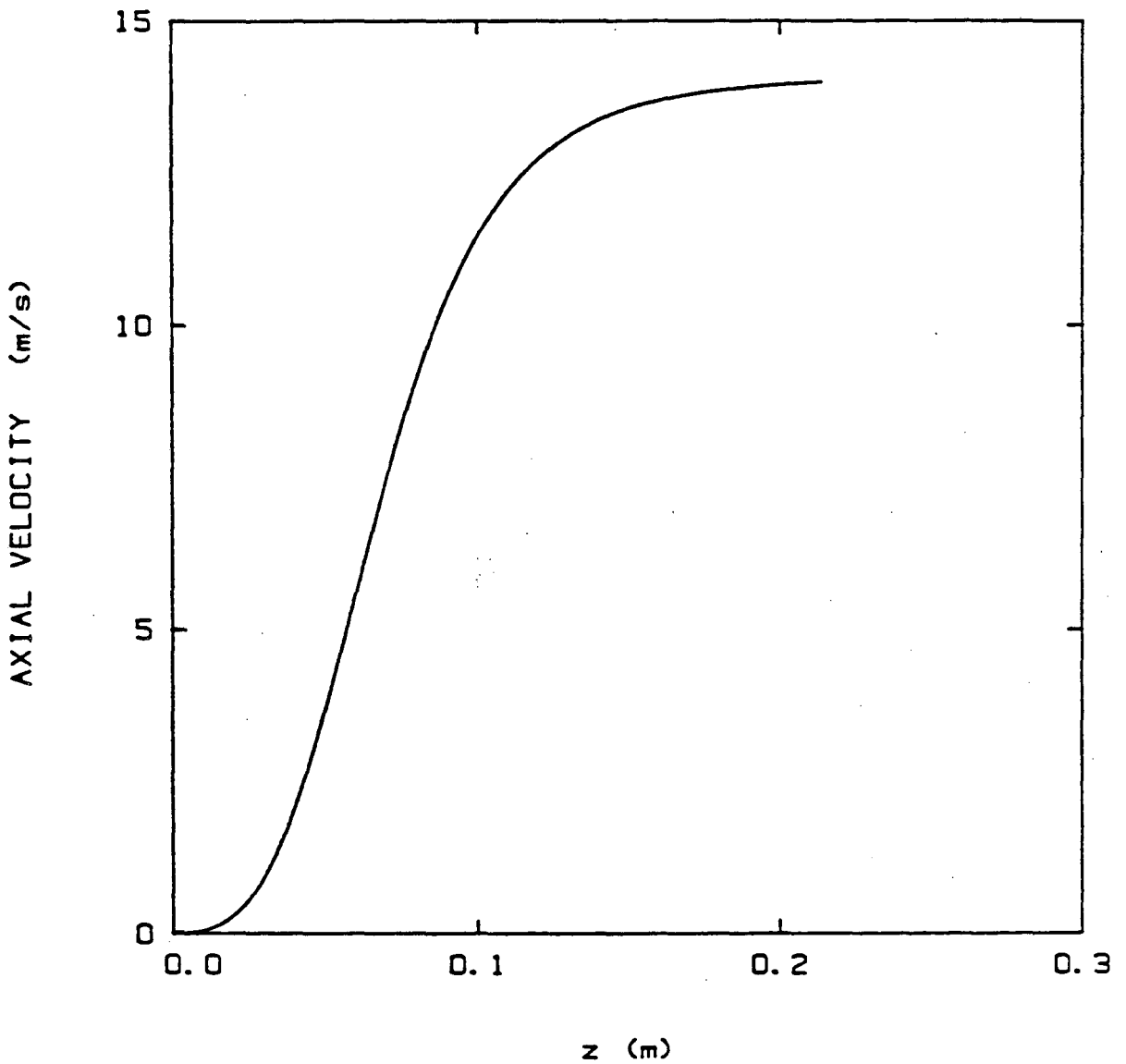

FIGURE 3.

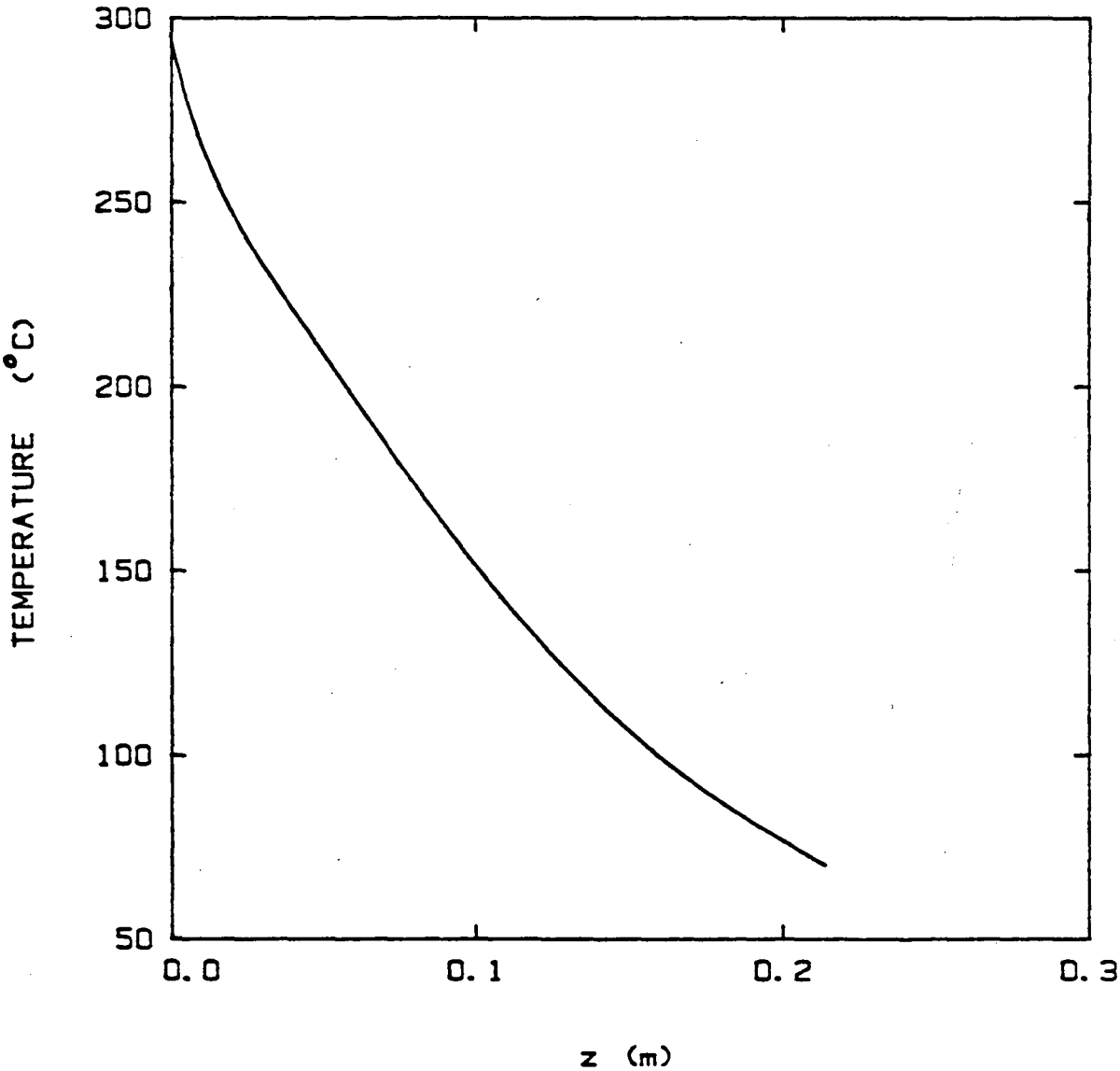

FIGURE 4.

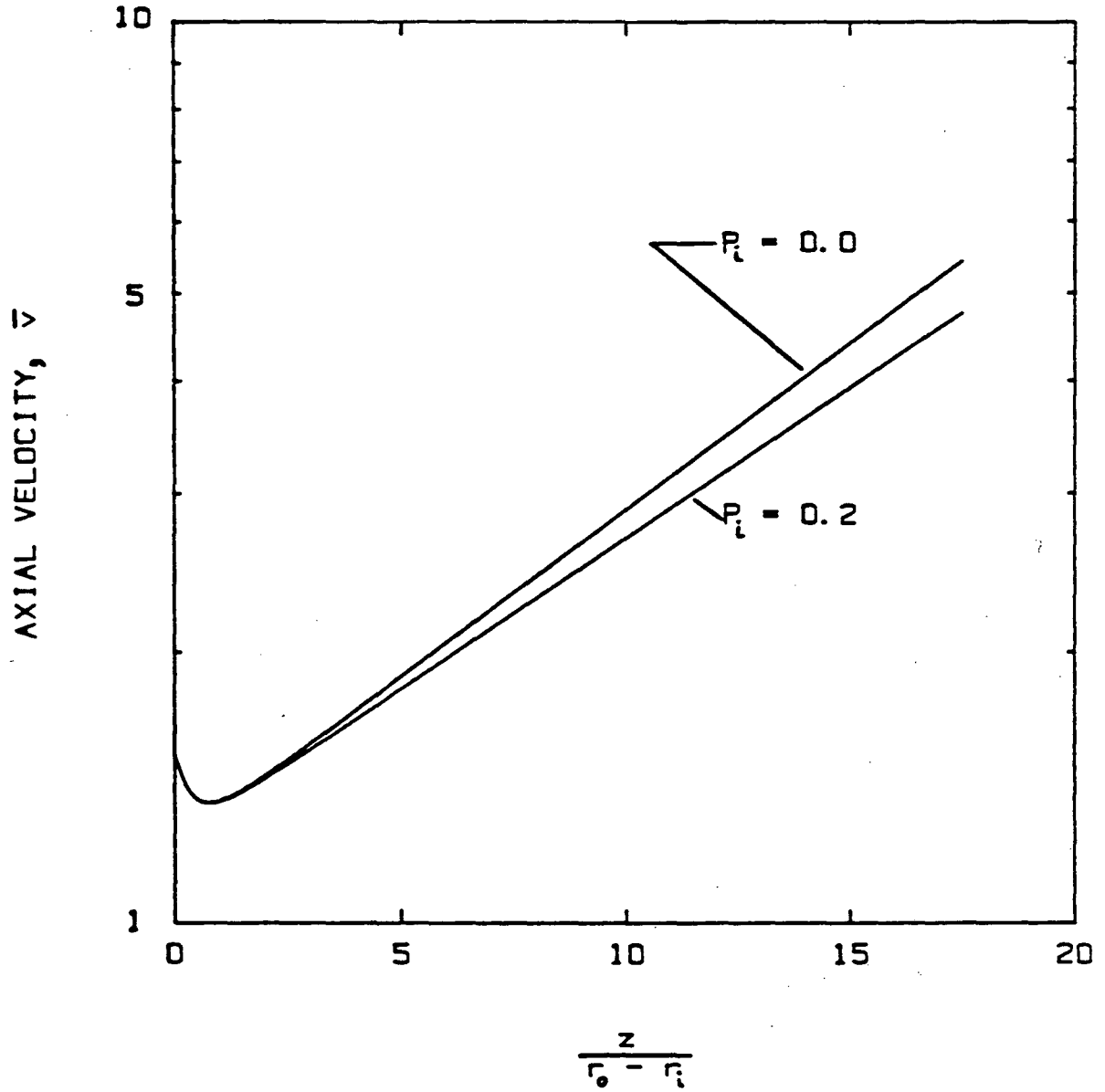

FIGURE 5.

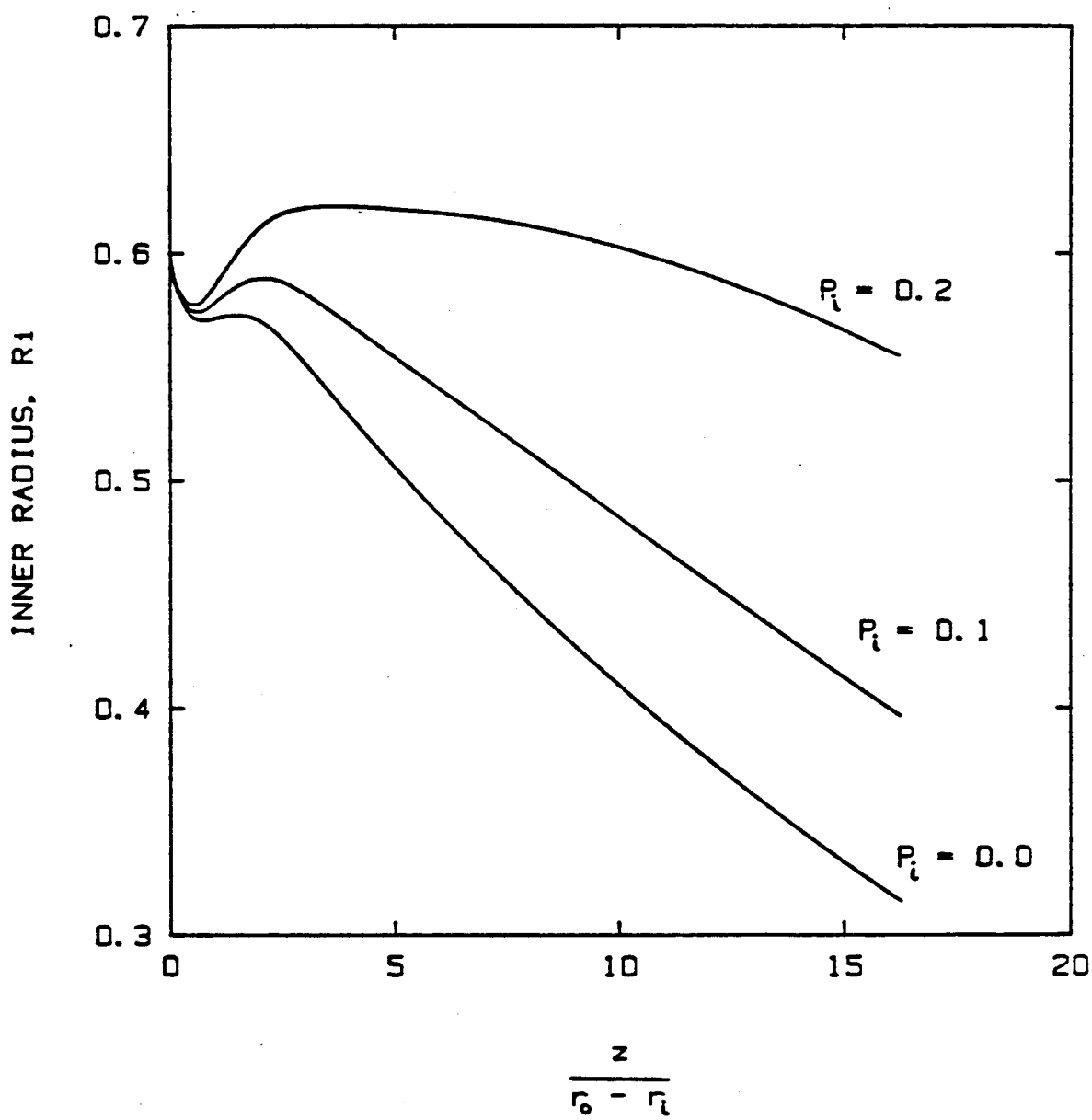
0.7
0.6
0.5
0.4
0.3
INNER RADIUS, R1
0
5
10
15
20
P_i = 0.2
P_i = 0.1
P_i = 0.0
$\frac{z}{r_o - r_i}$

FIGURE 6.

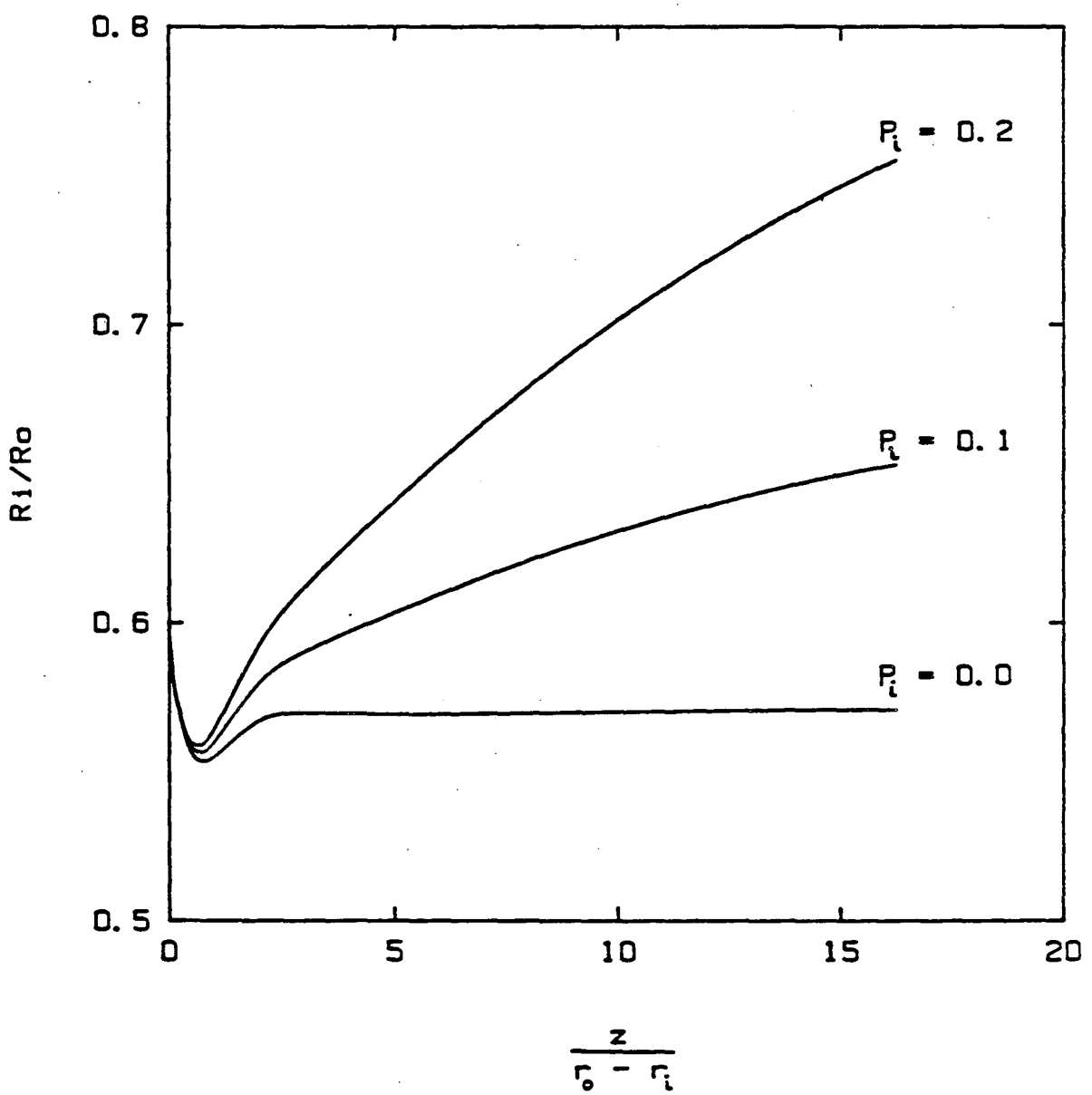

FIGURE 7.

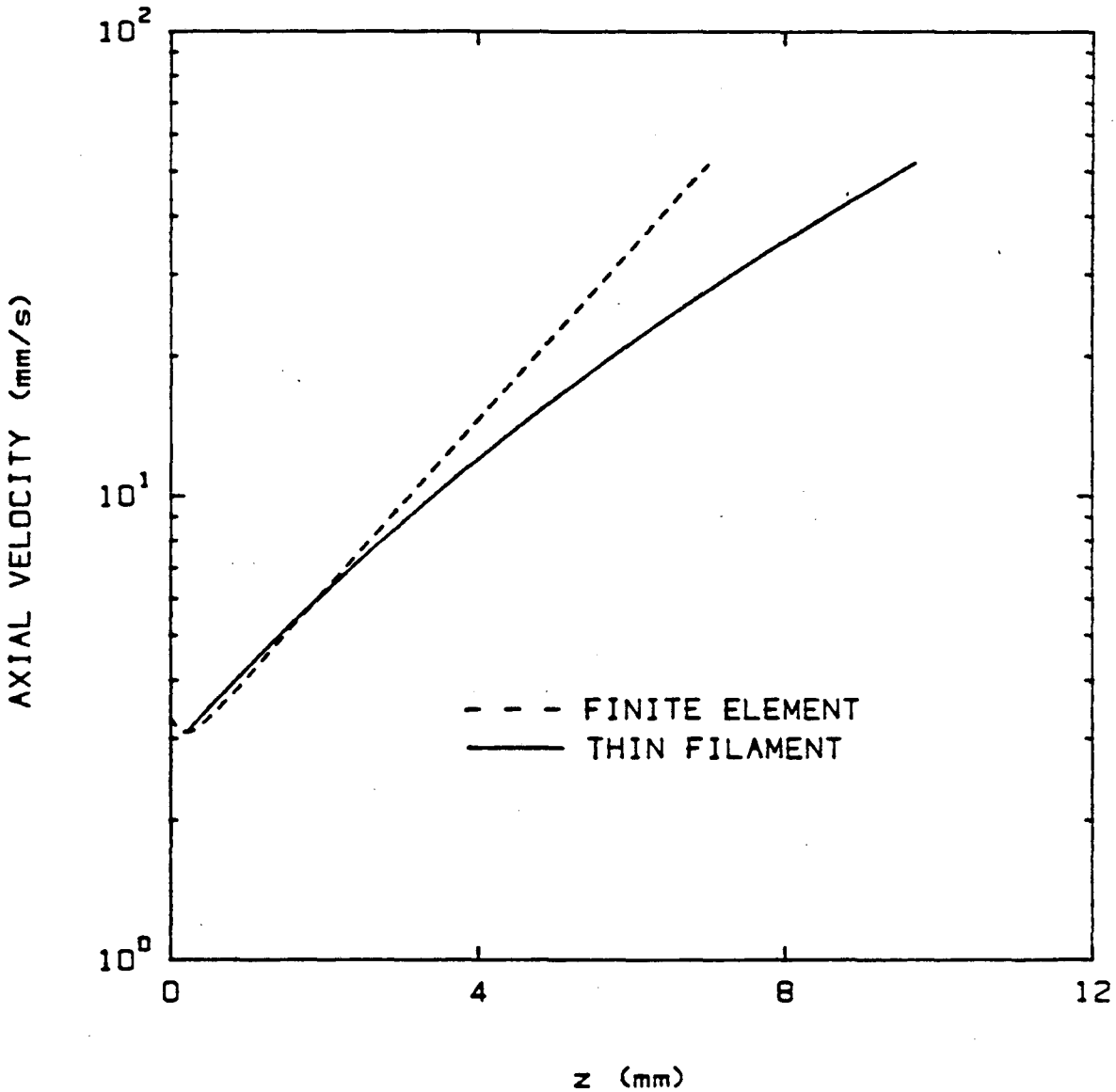
10^2
10^1
10^0
AXIAL VELOCITY (mm/s)
0
4
8
12
z (mm)
FINITE ELEMENT
THIN FILAMENT

FIGURE 8.

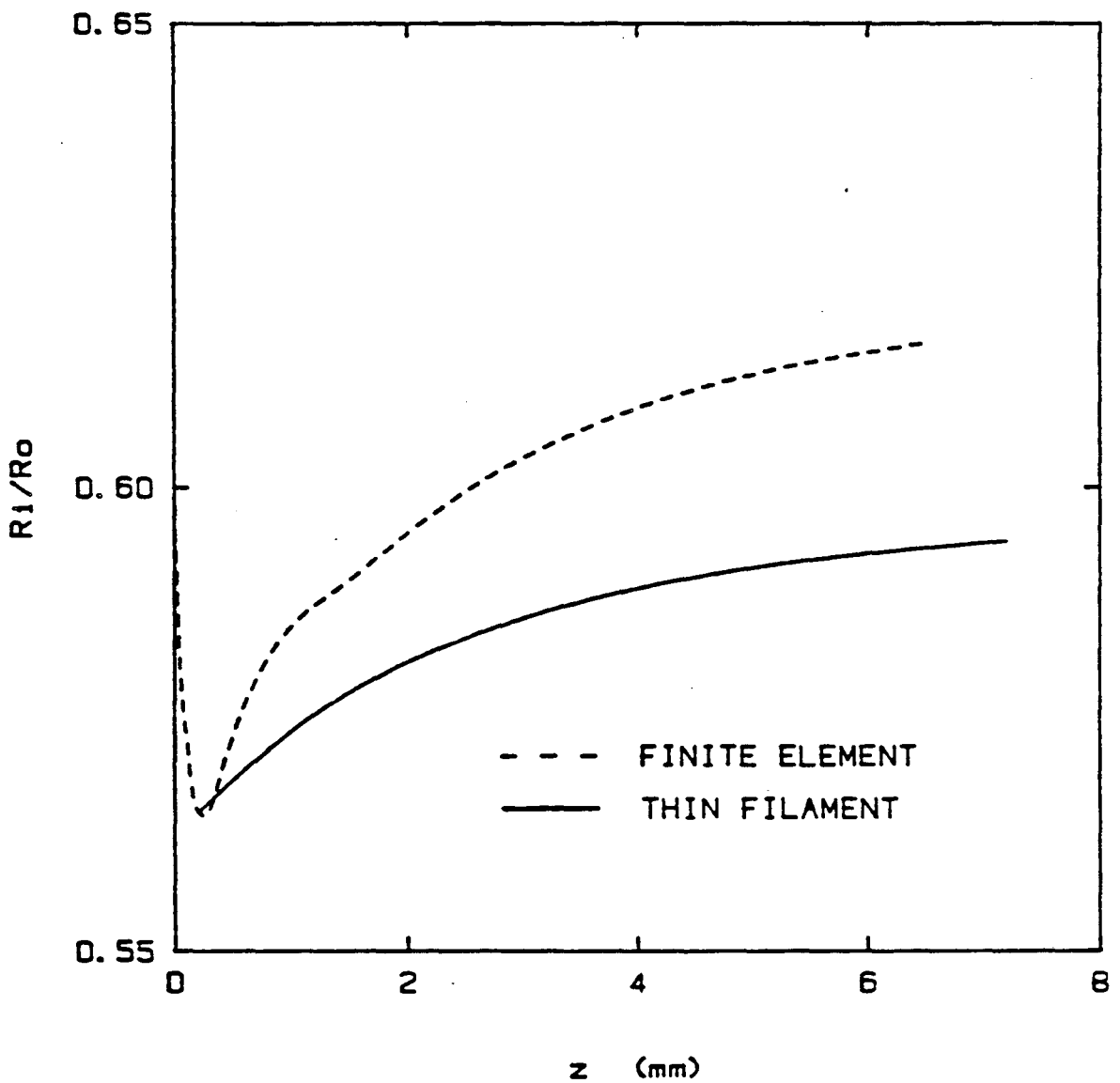

FIGURE 9.

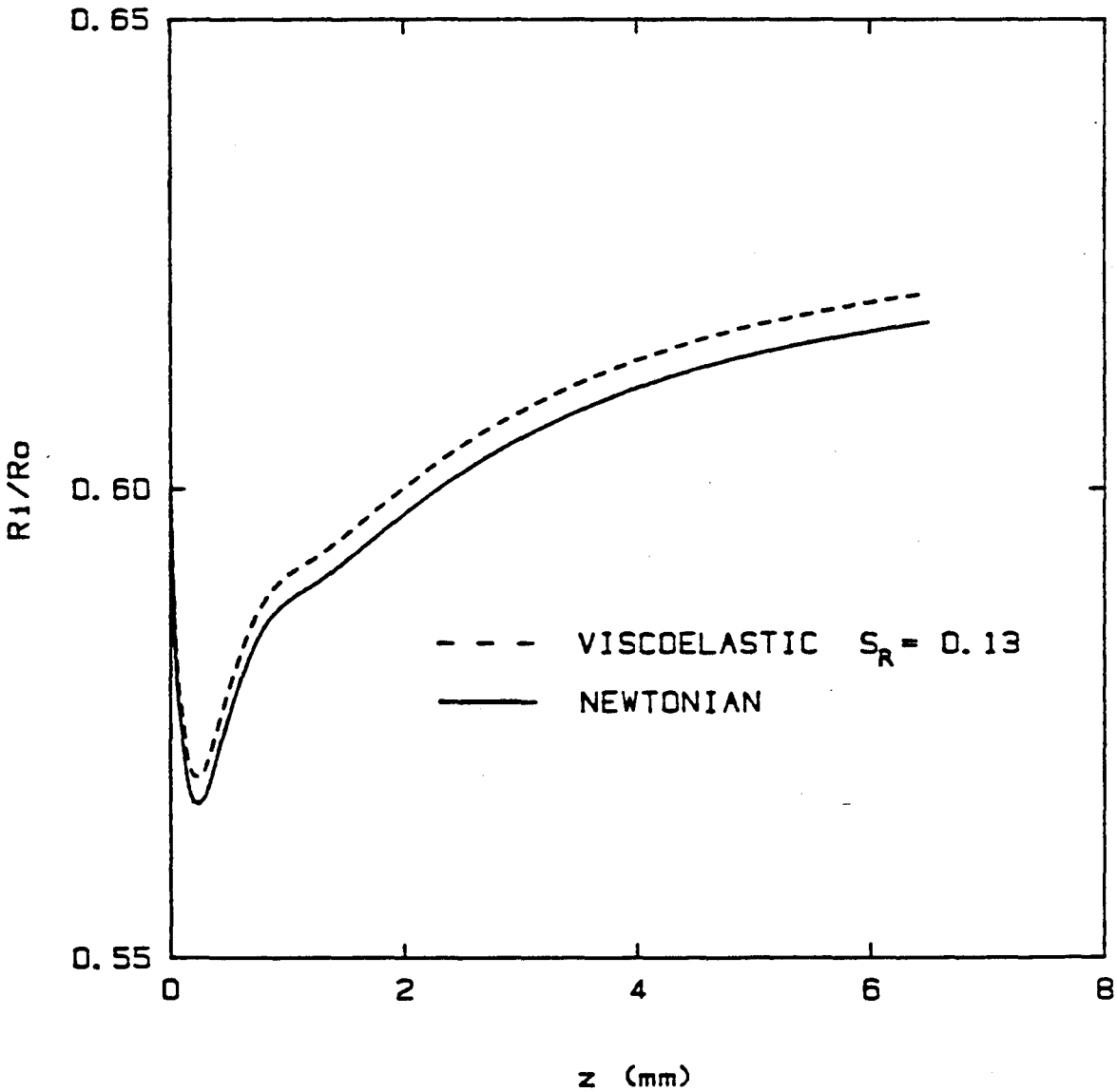

This report was done with support from the Department of Energy. Any conclusions or opinions expressed in this report represent solely those of the author(s) and not necessarily those of The Regents of the University of California, the Lawrence Berkeley Laboratory or the Department of Energy.

Reference to a company or product name does not imply approval or recommendation of the product by the University of California or the U.S. Department of Energy to the exclusion of others that may be suitable.

TECHNICAL INFORMATION DEPARTMENT
LAWRENCE BERKELEY LABORATORY
UNIVERSITY OF CALIFORNIA
BERKELEY, CALIFORNIA 94720